Laboratory study on vertical and horizontal resistance of the pile installed by various displacement pile installation methods

Shunsuke Moriyasu [i)], Xi Xiong [ii)], Shun-ichi Kobayashi [iii)] and Tatsunori Matsumoto [iv)]

i) Senior Researcher, Steel Structures Research Laboratory, NIPPON STEEL CORP., 20-1, Shintomi, Futtsu 293-8511, Japan.

ii) Associate professor, Faculty of Geoscience and Civil Engineering, Kanazawa University, Kakuma, Kanazawa 920-1192, Japan.

iii) Assistant professor, Faculty of Geoscience and Civil Engineering, Kanazawa University, Kakuma, Kanazawa 920-1192, Japan.

iv) Professor Emeritus of Kanazawa University, Kakuma, Kanazawa 920-1192, Japan.

ABSTRACT

In the regions where earthquakes occur frequently, to properly design the pile foundation, both the vertical and horizontal resistance of the pile should be considered. The objective of this study was to investigate the influence of pile installation methods on vertical and horizontal pile resistances. In a series of laboratory experiments, four types of pile installation methods were used: monotonic push-in, surging (repetitive push-in and pull-out), vibratory pile driving, and bored pile (non-displacement) methods. Additionally, two types of model piles with different flexural rigidities were used. Moreover, vertical and horizontal load tests were conducted, successively, on the model piles. Though the pile installed using the displacement pile methods showed higher vertical resistance than that of the pile installed using the bored pile method, their horizontal resistance was found to be almost the same.

Keywords: displacement pile installation method, laboratory experiment, vertical load test, horizontal load test

1 INTRODUCTION

In the regions where earthquakes occur frequently, the ultimate vertical bearing capacity of a pile foundation is usually designed to consider the force of an earthquake. Additionally, the foundation's horizontal resistance against the force of the earthquake is also important. Therefore, to properly design pile foundations, both the vertical and horizontal resistance of the pile should be considered.

It is widely known that displacement pile installation methods, such as the impact hammer method and push-in method, push away the soil surrounding the pile, and this increases the vertical bearing capacity of the pile, compared to non-displacement pile methods. The degree of the installation effect depends on the kind of displacement pile installation method used. This is usually considered in the design codes. For example, in the Specifications for highway bridges part IV (Japanese Road Association, 2017), the bearing capacity of the pile base is defined as $\alpha N A_p$, where α is a coefficient depending on the piling method, N is the SPT N-value (if N exceeds 50, $N = 50$), and A_p is the area of the pile base. The value of α is usually 130 for piles installed using the impact hammer method in a sandy area, whereas α = 110 is for piles installed using the bored pile method. The horizontal resistance of a pile installed using the displacement pile installation method is often the same as that of the corresponding non-displacement pile method. This means that the effect of the pile installation method is not considered in the design of horizontally loaded piles, but in design codes, the effect is considered for the vertical bearing capacity. Therefore, existing design codes may overestimate or underestimate the horizontal resistance of a pile installed using the displacement pile installation methods.

The objective of this study is to investigate the influence of displacement pile installation methods on both vertical and horizontal pile resistances. This study compares the vertical and horizontal resistances of piles installed using four types of pile installation methods: monotonic push-in, surging (repetitive push-in and pull-out), vibratory pile driving, and bored pile installation (non-displacement pile), through a series of laboratory experiments.

2 EXPERIMENTAL DESCRIPTION

In a series of laboratory experiments, a model pile was installed using four types of pile installation methods. After the pile penetration tests (PPTs) were conducted, the vertical load tests (VLTs), and the horizontal load tests (HLTs) were conducted successively. Finally, cone penetration tests (CPTs) were conducted to investigate the soil condition of each model ground.

To compare the influence of pile rigidity, high and low flexural rigidity piles, as shown in Fig. 1, were used. The high flexural rigidity pile (HRP) was a closed-ended aluminum pile with a diameter of 32 mm, a wall thickness of 1.3 mm, and a bending rigidity of 1,073 Nm^2. The low flexural rigidity pile (LRP), was a closed-ended aluminum plate pile with a width of 32 mm, a wall thickness of 4.0 mm, and a bending rigidity of 12.4 Nm^2. Both piles had a length of 600 mm. As shown in Fig. 1, strain gauges were attached to the pile shaft on opposite sides at each level to obtain the axial forces and bending moments. The pile surface with the strain gauges was coated with an acrylic adhesive and glued with silica sand #6, which was also used for the model ground.

The model ground material was dry silica sand #6. Its physical properties are listed in Table 1. The model ground was prepared with 12 layers of sand (11 layers were 50 mm thick and 1 layer was 30 mm) in a cylindrical soil container with an inner diameter and a height of 566 and 580 mm, respectively. The sand was compacted using a small tamper to adjust the relative density, D_r, to 80 %.

Table 2 lists the experimental cases. In total, eight cases were considered. During the PPTs, the model pile was pushed into the model ground until the pile head displacement, w_h, reached approximately 410 mm. In the cases of monotonic push-in and surging, the model pile was installed at a penetration rate of 0.2 mm/s using an electrical jack (see Fig. 2). In the cases of surging, the pile was installed with repetitions of 4 mm push-in and 2 mm pull-out strokes.

Table 1. Physical properties of silica sand #6.

Minimum dry density, ρ_{dmin}	(t/m^3)	1.37
Maximum dry density, ρ_{dmax}	(t/m^3)	1.63
Maximum void ratio, e_{max}		0.96
Minimum void ratio, e_{min}		0.65
Mean particle size, D_{50}	(mm)	0.51

Table 2. Experimental conditions.

Case	Pile flexural rigidity	Pile installation method
Case 1	High flexural rigidity pile (HRP)	Monotonic push-in
Case 2	High flexural rigidity pile (HRP)	Surging
Case 3	High flexural rigidity pile (HRP)	Vibratory pile driving
Case 4	High flexural rigidity pile (HRP)	Bored pile installation
Case 5	Low flexural rigidity pile (LRP)	Monotonic push-in
Case 6	Low flexural rigidity pile (LRP)	Surging
Case 7	Low flexural rigidity pile (LRP)	Vibratory pile driving
Case 8	Low flexural rigidity pile (LRP)	Bored pile installation

During PPT, the pile head load, P_h, was measured using a load cell between the pile head and the jack. In the cases of vibratory pile driving, a vibratory hammer model with a weight of 275 N and a maximum frequency of 60 Hz was employed (see Fig. 2). When the two motors rotated eccentric masses in opposite directions, the horizontal vibrations were negated, and the vertical vibrations were harmonized. At the beginning of the PPT in the vibration cases, the pile was installed using the hammer weight alone. When the pile could not be installed using the hammer weight alone, a vibration was started at a low frequency (low power). Additionally, when the pile penetration stopped, the vibration frequency was increased to improve the pile installation. P_h was the axial force near the pile top (SG 1 in Fig. 1) minus the inertial force of the pile body, which was calculated from the product of the pile mass and acceleration measured near the pile top. In the case of bored (buried) piles, the pile was embedded during the model ground preparation.

Subsequently, the VLTs were conducted. In all cases, the pile head was pushed down by the electrical jack at a rate of 0.1 mm/s. P_h was measured using the load cell between the pile head and the jack.

After the jack force during the VLTs was unloaded, the HLTs were conducted. As shown in Fig. 3 and Fig. 4, a wire connected to the pile head was pulled using a hand winch. The horizontal load, H, was measured using a load cell connected between the wire and the winch. To avoid the influence of preloading, the displacement control manner was adopted at the beginning of loading.

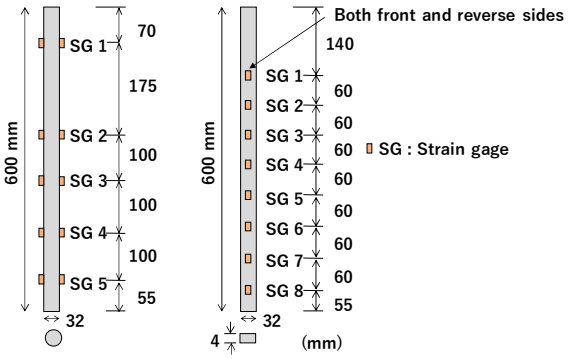

Fig. 1. Model piles (left: HRP, right: LRP).

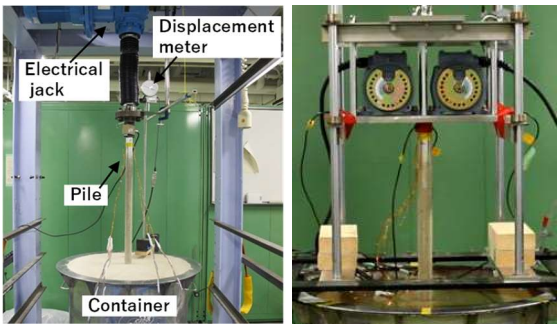

Fig. 2. Loading apparatus (left: PPTs in push-in and surging cases, and the VLTs in all the cases; right: PPTs in vibration cases).

Because the Specifications for highway bridges part IV (Japanese Road Association, 2017) allows a lateral pile displacement 1.0 ~ 3.8 % of the pile diameter, the pile in this experiment was loaded until the horizontal pile displacement over 3.8 % of the pile diameter. The horizontal displacement and inclination of the pile head were measured using a dial gage displacement meter and an accelerometer, respectively. Finally, the CPTs were conducted at four locations, as shown in Fig. 5, to measure the influences on the surrounding ground.

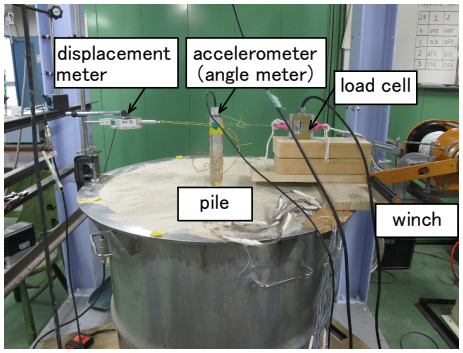

Fig. 3. Loading apparatus: HLTs.

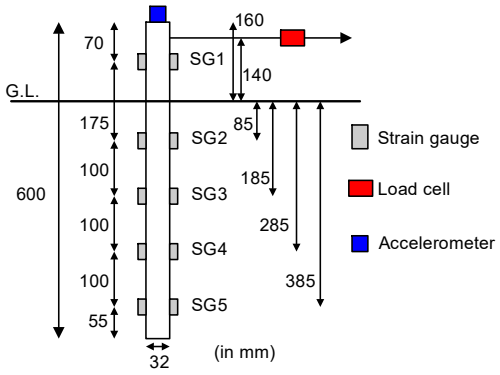

Fig. 4. Schematic diagram of the HLTs.

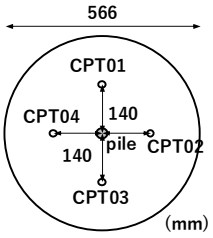

Fig. 5. Locations of the CPTs.

3 EXPERIMENTAL RESULTS

3.1 Results of pile penetration tests and vertical load tests

Fig. 6 (a) shows the relationship between P_h and w_h values in the PPTs for the displacement pile method cases. The P_h values in the HRP cases (cases 1, 2, and 3) are higher than those in the LRP cases (cases 5, 6, and 7). Figs. 6 (b) and (c) show the relationship between P_h and w_h values during the VLTs. In the HRP cases, the P_h values in all the displacement pile cases (cases 1, 2 and 3) are higher than those in the bored pile case (case 4) (see Fig. 6 (b)). This indicates that the pile installed during the PPTs improved the strength of the soil surrounding the pile. Additionally, the P_h in case 3 suddenly dropped during w_h = 435–437 mm after P_h reached its peak. Moriyasu et al. (2020) pointed out that a large number of cyclic pile movements during vibratory pile driving form a densified soil zone around the pile and a relatively loose outer soil zone (see Fig. 7). If such a ground condition is formed, the P_h at the beginning of a VLT becomes high owing to the densified soil zone. After the pile is displaced by a large amount of w_h during the VLT, the densified soil zone reaches critical state, and the outer soil zone contributes to soil resistance. If the soil strength of the outer zone is less than that of the densified zone, then the P_h may decrease.

However, this effect would not be notable in the LRP cases. Differences between the P_h in all the displacement pile method cases (cases 5, 6, and 7) and in the bored pile method case (case 8) are not noticeable (see Fig. 6 (c)).

Fig. 8 shows the relationship between the pile head load at the end of the PPTs, P_{h_PPT}, and the maximum pile head load at a 5 mm pile head displacement during the VLTs, P_{h_VLT}. The P_{h_VLT} of the 5 mm displacement was selected because the P_h during the VLTs reached the yield point within the 5 mm penetration. Only in case 3 (vibration), P_{h_VLT} was selected as 4,577 kN over 5 mm pile head displacement, because P_h converged after the peak value 5,625 kN at w_h = 435 mm (see Fig. 6b).

In case 1, the P_h obtained during the VLTs is smaller than that obtained during the PPTs. This could be because the pile penetration rate was slower during the VLTs than in the PPTs. In case 3, P_h during the VLTs is higher than during the PPTs. Moriyasu et al. (2020) reported that during a PPT, the movement of the cyclic pile generates a soil contraction around the pile, and this decreases the P_h. When the cyclic pile movement during PPTs changes to a monotonic movement during VLTs, the soil contraction turns into a soil dilation. A similar phenomenon appeared in this case. In case 2, the relationship between P_h during PPTs and that during VLTs is the result of both effects, i.e., the change in pile penetration rate, and the change in cyclic pile movement to monotonic movement. These differences among the three pile installation methods are not as considerable in the LRP cases, because the P_h during the VLTs is almost the same as that during the PPTs (see Fig. 8).

Fig. 9 shows the ratio of each pile resistance to that of the bored pile during the VLTs. The horizontal axis is the pile base resistance ratio of each displacement pile to the bored pile. The vertical axis is the ratio of the pile shaft resistance of each pile to that of the bored pile. It can be seen from Fig. 9 that the pile base in HRP cases is higher than that in the LRP cases. This indicates that the large installed pile volume in cases 1, 2, and 3 strengthened the soil resistance surrounding the pile tip.

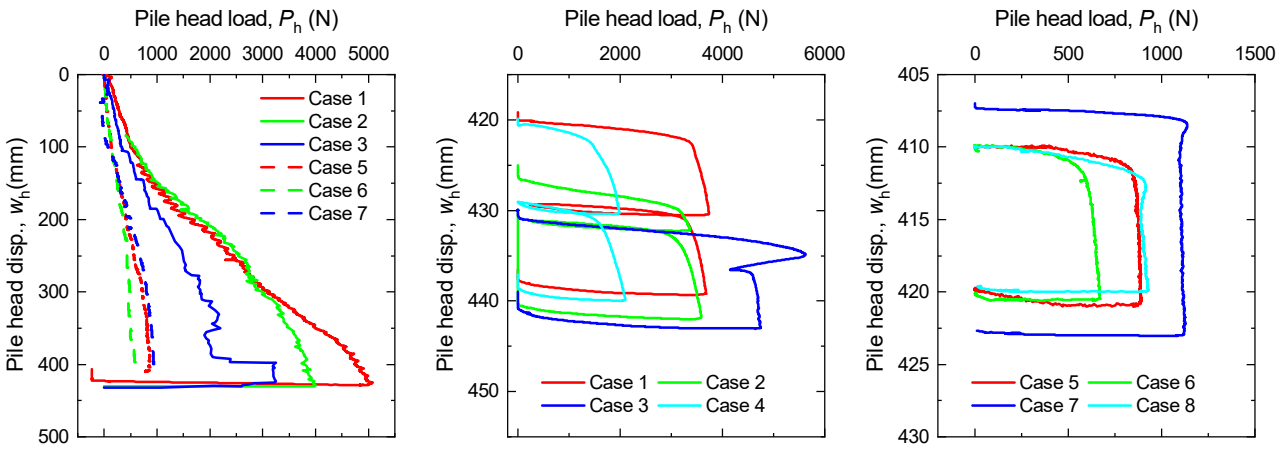

(a) P_h – w_h relation during PPT in all cases (b) P_h – w_h relation during VLT in HRP cases (c) P_h – w_h relation during VLT in LRP cases
Fig. 6. Relationship between the pile head load, P_h, and pile head displacement, w_h, during the PPTs and VLTs.

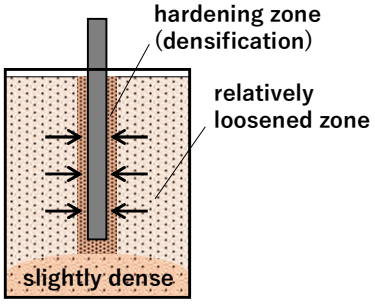

Fig. 7. Schematic of the soil condition in case 3 (vibration).

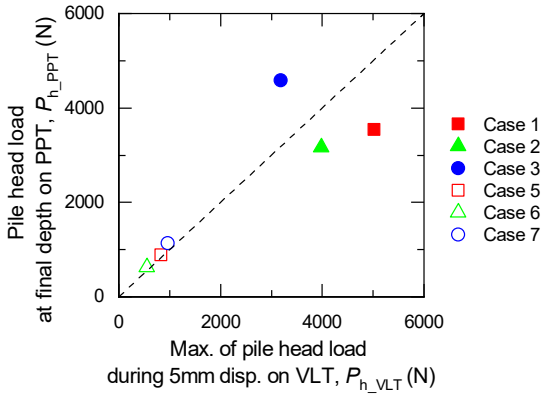

Fig. 8. Relationship between the pile head load at final depth during the PPTs, P_{h_PPT}, and the maximum pile head load at 5 mm pile head displacement during the VLTs, P_{h_VLT}.

In the next, we shall discuss the pile shaft resistance ratio. As shown in the vertical axis of Fig. 9, the ratios in cases 1 and 2 are approximately 1.2, and those in cases 5 and 6 are less than 1.0. These relatively small ratios mean that the influence of the pile installation method is not noticeable. On the other hand, the ratios in cases 3 and 7 are the highest in the HRP and LRP cases, respectively. This result corresponds to the soil density distribution shown in Fig. 7. The densified soil zone surrounding the pile, caused by a large number of cyclic pile movements during vibratory pile driving, would increase the pile shaft resistance during VLT.

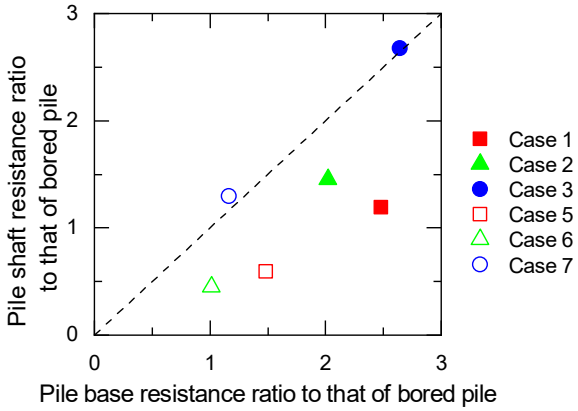

Fig. 9. Pile base and shaft resistance ratios of the displacement pile cases to that of the bored pile case.

3.2 Results of horizontal load tests

Fig. 10 shows the results of the HLTs for the HRP cases. Because the horizontal load in cases 1 and 2 is higher than that in case 4, the horizontal soil resistances in these cases are observed to be influenced by the strengthening effect that the displacement pile has on the soil resistance surrounding the pile (see Fig. 10 (a)). In case 3, the horizontal load is the same as in case 4, indicating that the effect has not influenced the horizontal resistance.

Fig. 10 (b) compares the pile deflection distribution when the horizontal pile head displacement during the HLTs, u, reached 5 mm. The pile deflection was calculated from the measured pile bending strains, pile top displacement, and pile top inclination. Therefore, it can be seen from Fig. 10 (b) that the piles are rotated relatively deep at depth z from the ground surface. The rotation centers in cases 1, 2, and 4 are within the range of z = 160–200 mm, whereas that in case 3 is z = 250 mm. Near the pile base (z = 430 mm), the pile deflection in cases 1, 2, and 3 is much smaller than that in case 4. As mentioned in Section 3.1, the large volume of the installed pile would increase the pile base resistance in

the vertical direction. Associated with it, the horizontal resistance around the pile base would also increase during PPTs.

Fig. 10 (c) shows the soil pressure distributions, which were obtained from the bending moments. Soil pressures in this figure mean the difference in pressures, i.e., those acting on the front side (loading direction) of the pile, are subtracted by those on the back side. It can be seen from Fig. 10 (c) that the minimum soil pressure in cases 1 and 2 is greater than that in case 4. This indicates that horizontal stiffness was increased due to soil compaction of a surrounding ground during pile penetration. Regarding case 3, the minimum soil pressure (z = 300 mm) is deeper than in other cases (z = 100–200 mm). The soil pressure distribution in case 3 is also different from that in the other cases, which might be due to the disturbance of the shallow soils during vibratory installation. This means that the horizontal soil resistance at the shallow depth in case 3 is smaller than that in other cases. As a result, case 3 shows a similar horizontal stiffness compared to case 4.

Fig. 11 (a) shows the relationship between the horizontal pile head displacement and the horizontal load of the HLTs for the LRP cases. Compared to the initial stiffness of the HRP cases, the differences between the displacement pile cases 5 to 7 and the bored pile method (case 8) are small. As shown in Fig. 11 (b), the pile deflection in the displacement pile cases is larger than that in the bored pile case (case 4). The soil pressure distribution of case 8 is slightly different from that in cases 5, 6, and 7, but they are almost similar as shown in Fig. 11(c).

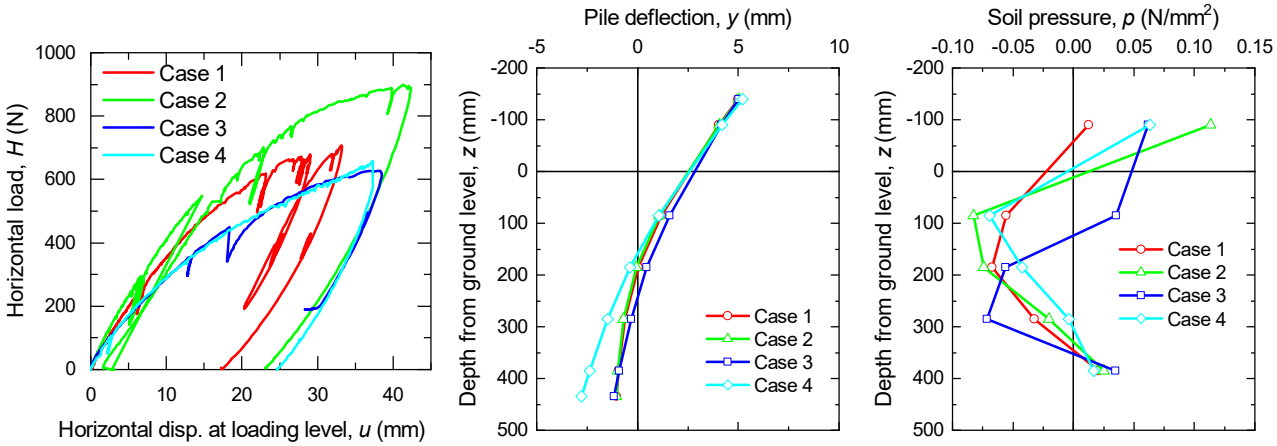

(a) Relationship between H and u (b) Pile deflection at u = 5 mm. (c) Soil pressure on the pile at u = 5 mm.

Fig. 10. HLT results of the HRP cases.

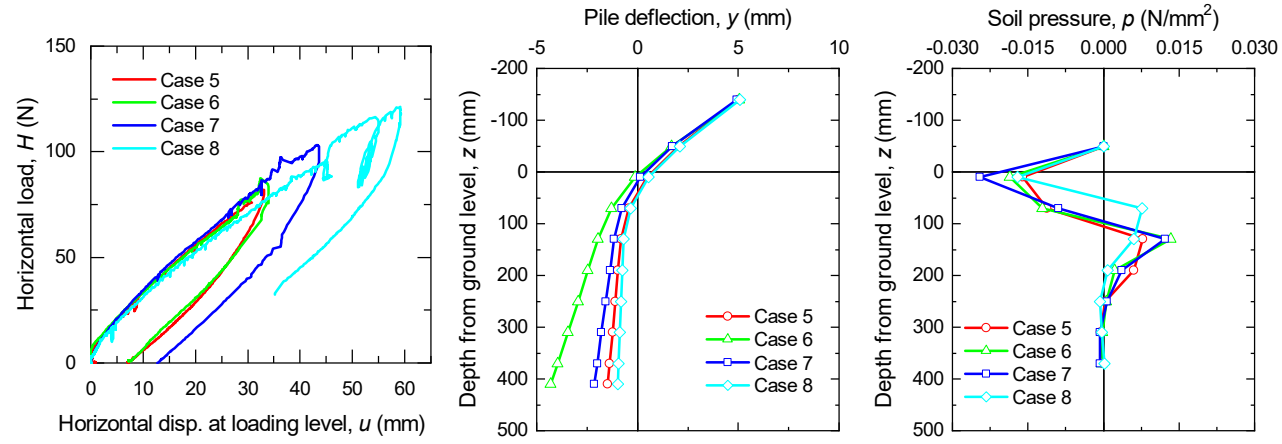

(a) Relationship between H and u (b) Pile deflection at u = 5. mm. (c) Soil pressure on the pile at u = 5 mm.

Fig. 11. HLT Results of the LRP cases.

3.3 Results of cone penetration tests

Fig. 12 shows the distributions with depth of the CPT tip resistance, q_t. Each line represents the average q_t at the four CPT locations, as shown in Fig. 5, for each case. It can be seen from Fig. 12 (a) that the values of q_t in cases 1, 2, and 3 are higher than in case 4 (bored pile). Because CPTs were carried out after the PPTs, VLTs, and HLTs, the pile installation in cases 1, 2 and 3 (displacement pile cases) would have increased the strength of the soil around the pile. Furthermore, the q_t values in in cases 1, 2, and 3 are higher than those in cases 5 to 8 (see Figs. 12 (a) and (b)). These CPT results

support the presumption that the large volume of installed pile in cases 1, 2, and 3 would have increased the soil strength around the pile.

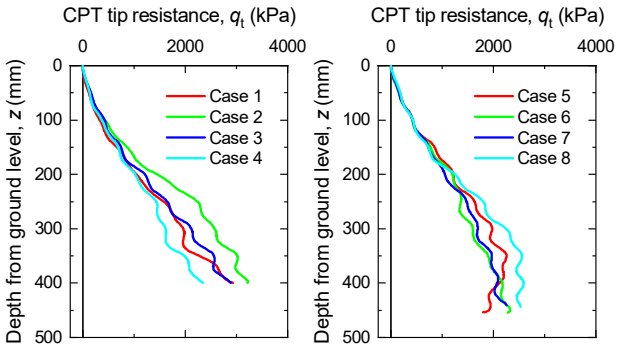

(a) cases 1 to 4 (b) cases 5 to 8

Fig. 12. Results of the CPTs.

3.4 Relationship between the vertical bearing capacity and the horizontal load resistance

Fig. 13 summarizes the effect of the displacement pile methods on the vertical and horizontal resistance. The vertical axis shows the ratio of the vertical pile head resistance in the displacement pile cases to that in the bored pile case during the VLTs. The vertical pile head resistance in each case is the same as the P_{h_VLT} defined in Section 3.1, i.e., P_{h_VLT} is the maximum pile head load within the 5 mm pile head displacement during the VLTs. However, in case 3, the P_{h_VLT} is the converged value over the 5 mm pile head displacement, after the peak value was dropped (see Fig. 6b). The horizontal axis is the ratio of the horizontal load, H, in the displacement pile cases to that in the bored pile case when the pile head displacement at the loading level reached 30 mm. Regarding the vertical resistance, the ratio in the HRP cases is much higher than that in the LRP cases. On the other hand, for the horizontal resistance, the ratio in the HRP cases is almost the same as that in the LRP cases. This means that the strengthening effect that the installed pile has on the soil resistance is significant in the vertical resistance of the HRP cases. This effect could be enhanced by using a larger pile tip area in the HRP cases. Moreover, the effect does not affect the horizontal resistance because the differences between the ratio in the HRP and LRP cases are negligible.

4 CONCLUSIONS

The objective of this study was to investigate the influence of displacement pile installation methods on vertical and horizontal pile resistances. In a series of laboratory experiments, four types of pile installation methods were used: monotonic push-in, surging (repetitive push-in and pull-out), vibratory pile driving, and bored pile installation (non-displacement pile). Additionally, the pile penetration tests (PPTs), vertical load tests (VLTs), and horizontal load tests (HLTs) were performed, successively, using two types of model piles (a closed-ended pipe pile with high flexural rigidity and a large pile tip area; and a plate pile with low flexural rigidity and a small pile tip area). The main findings of this study are as follows.

1) The results of the model experiment show that the soil resistance adjacent to the piles increased after the installation of the HRP displacement piles owing to the larger volume of soils displaced during the installation. This increase was not observed for the LRP displacement pile cases.
2) The vertical resistance of the displacement model piles is significantly larger than that of the bored model piles, whereas the horizontal resistance is almost similar among the displacement and bored model piles.
3) The results of this study strongly support Japanese Specification for highway bridges part IV (Japanese Road Association, 2017), which specifies using common design values for the horizontal resistance of a pile, regardless of piling methods used.

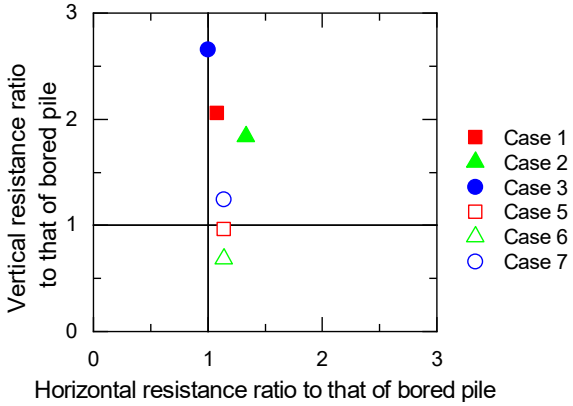

Fig. 13. Horizontal and vertical resistance ratio of the displacement pile cases to that of the bored pile case.

ACKNOWLEDGEMENTS

The authors would like to thank Mr. S. Shinomo (Kanazawa University), Ms. M. Ikeda, and Mr. D. Yoshioka (former students) for their assistance in this study.

REFERENCES

1) Japan Road Association (2017): Specifications for highway bridges part IV, *ISBN 978-4889502824*, 239, 254 (in Japanese).

2) Moriyasu, S., Matsumoto, T., Aizawa, M., Kobayashi, S. and Shimono, S. (2020): Effects of cyclic behaviour during pile penetration on pile performance in model load tests, *Geotechnical Engineering Journal of the SEAGS & AGSSEA*, 51(2), 150–158.